Kumaran

Figure 10: $\Gamma_c(H-1)^{0.75}$ (10(a)); $k_c(H-1)^{0.75}$ (10(b)); and $-s_{Ic}(H-1)^{0.5}$ (10(c)) as a function of Λ for $\eta_r = 0$ and $(H-1) \ll 1$. The solid line is the numerically determined critical velocity, and the broken line is the empirical relation given in Table 1 for $\Lambda > 0$.

Figure 11: The critical velocity Γ_c (11(a)); the wave number of the most unstable mode k_c (11(b)); and the frequency of the most ustable mode $-s_{Ic}$ (11(c)) as a function of Λ for $\eta_r = 0$ and $H \gg 1$. The solid line is the numerically determined critical velocity, and the broken line is the empirical relation given in Table 1 for $\Lambda \gg 1$.

Figure 12: The critical velocity Γ_c (12(a)); the wave number of the most unstable mode $k_c(H-1)$ (12(b)); and the frequency of the most ustable mode $-s_{Ic}$ (12(c))as a function of $(1-\eta_r)$ for $(H-1) \ll 1$ and $\Lambda = 0$. The solid line is the numerically determined critical velocity, and the broken line is the empirical relation given in Table 3 for $(1-\eta_r) \ll 1$.

Figure 13: The critical velocity Γ_c (13(a)); the wave number of the most unstable mode k_c (13(b)); and the frequency of the most ustable mode $-s_{Ic}$ (13(c))as a function of η_r of $H \gg 1$ and $\Lambda = 0$. The solid line is the numerically determined critical velocity, and the broken line is the empirical relation given in Table 3 for $\eta_r \gg 1$.

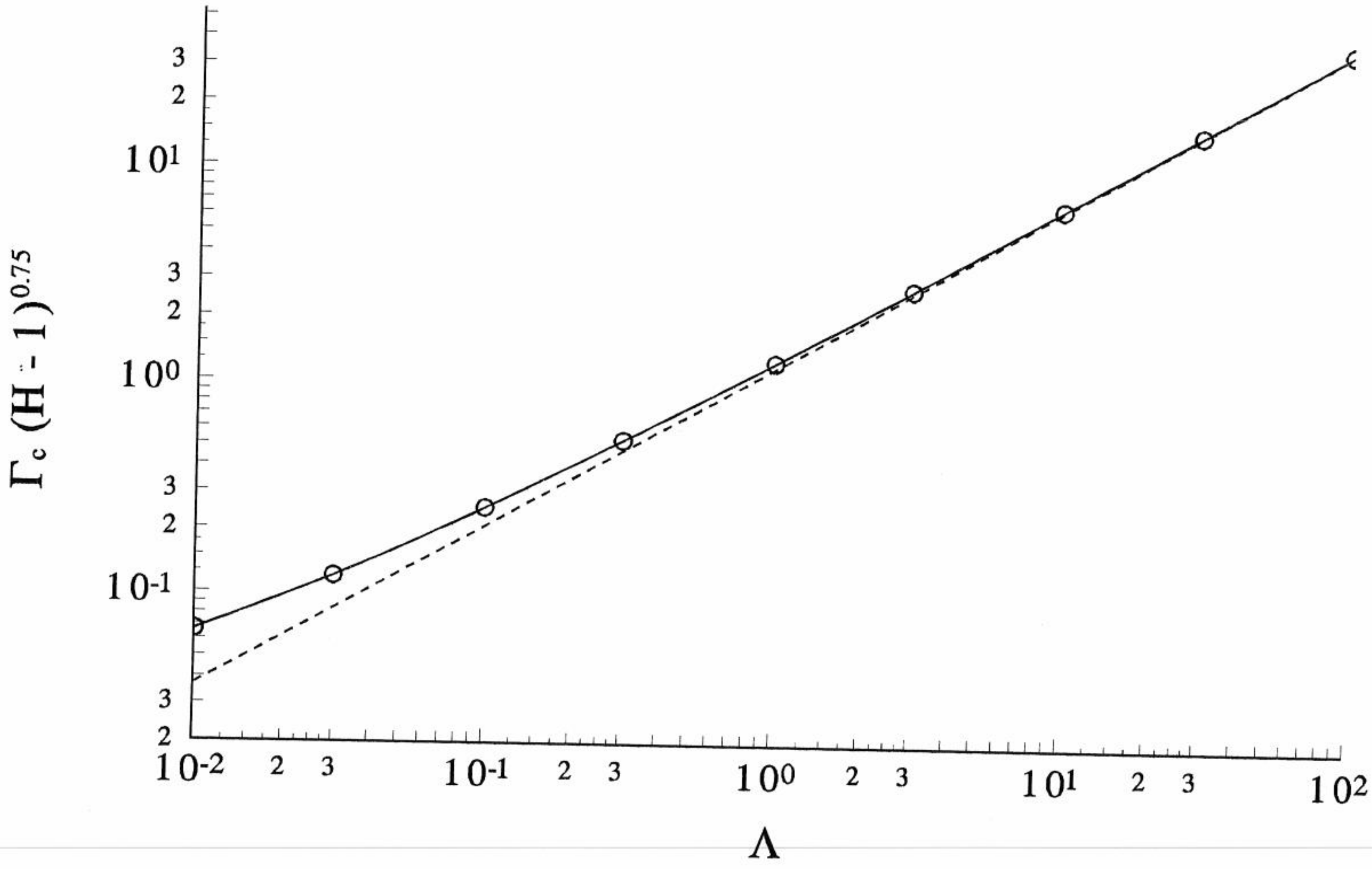

FIGURE 10(a)

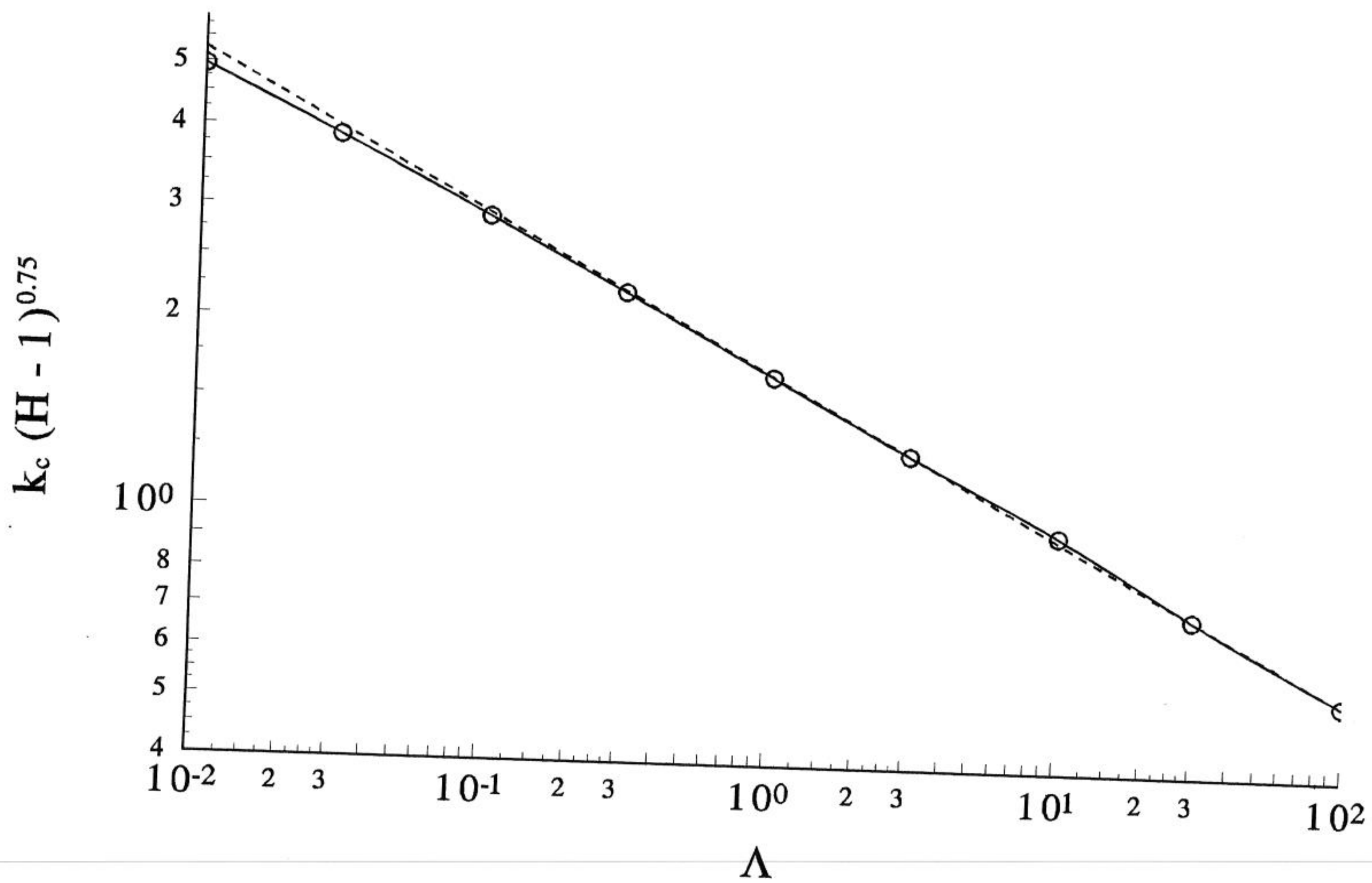

FIGURE 10(b)

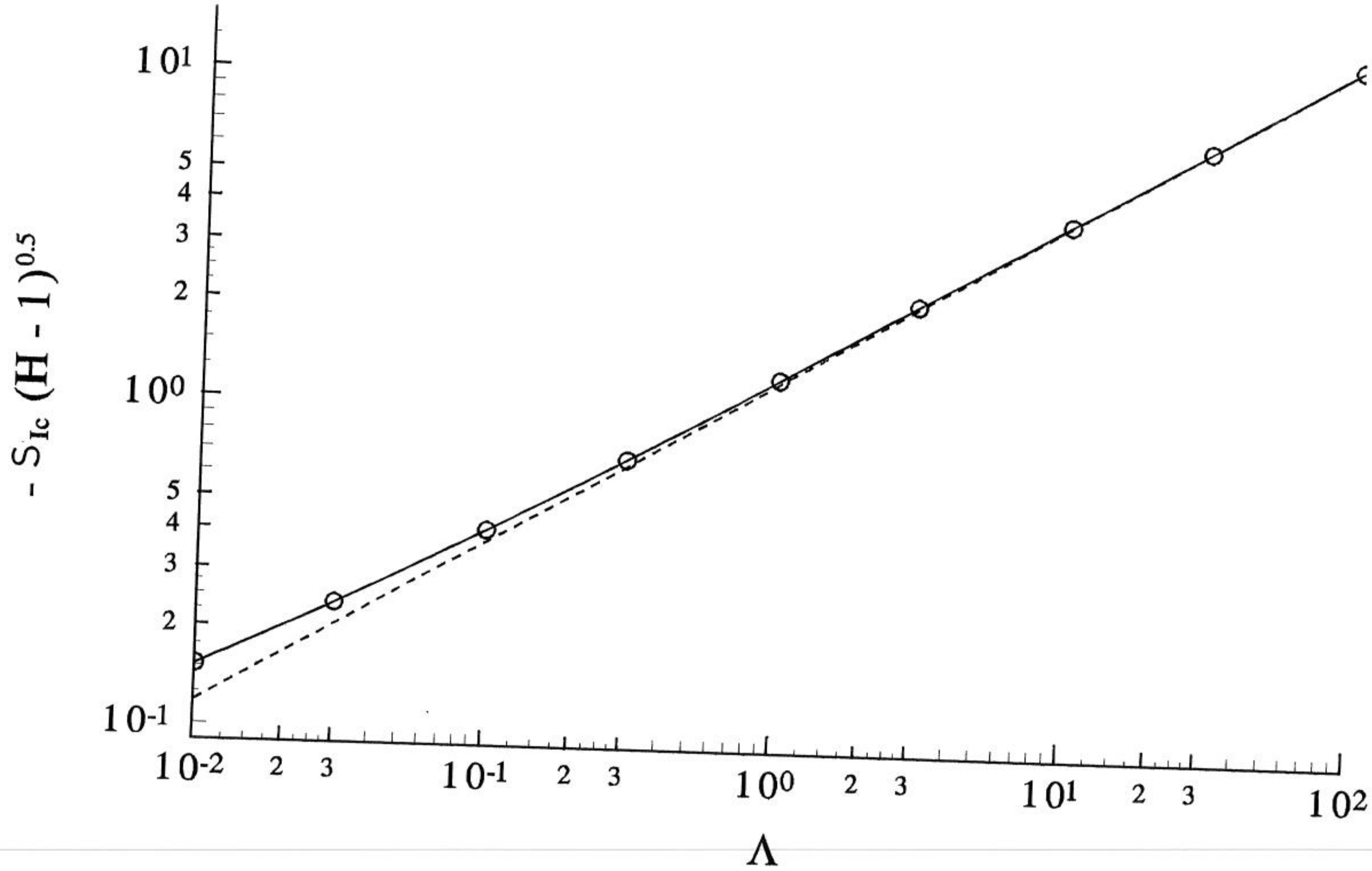

FIGURE 10(c)

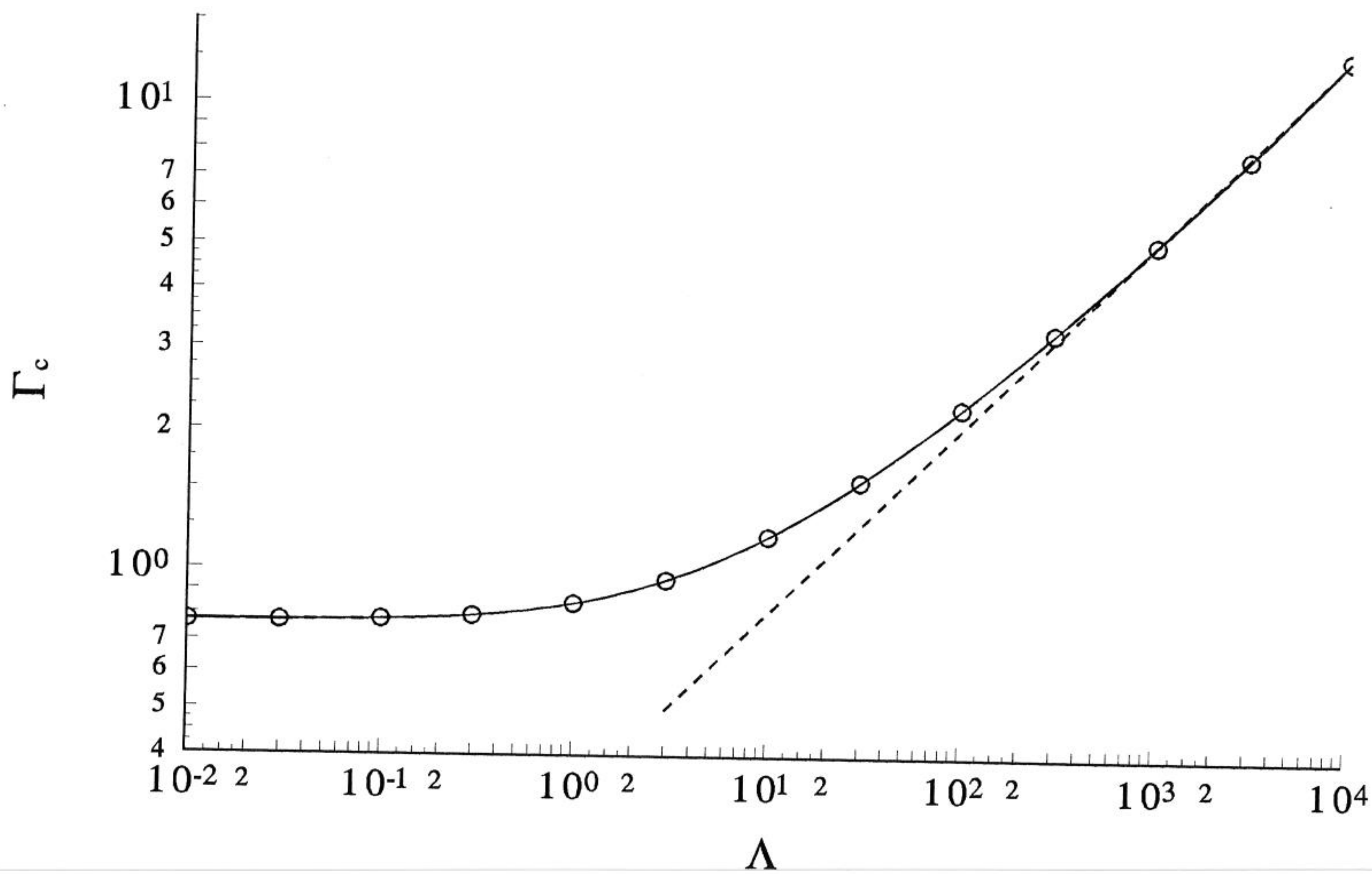

Γ_c
10^1
7
6
5
4
3
2
10^0
7
6
5
4
10^{-2} 2
10^{-1} 2
10^0 2
10^1 2
10^2 2
10^3 2
10^4
Λ

FIGURE 11(a)

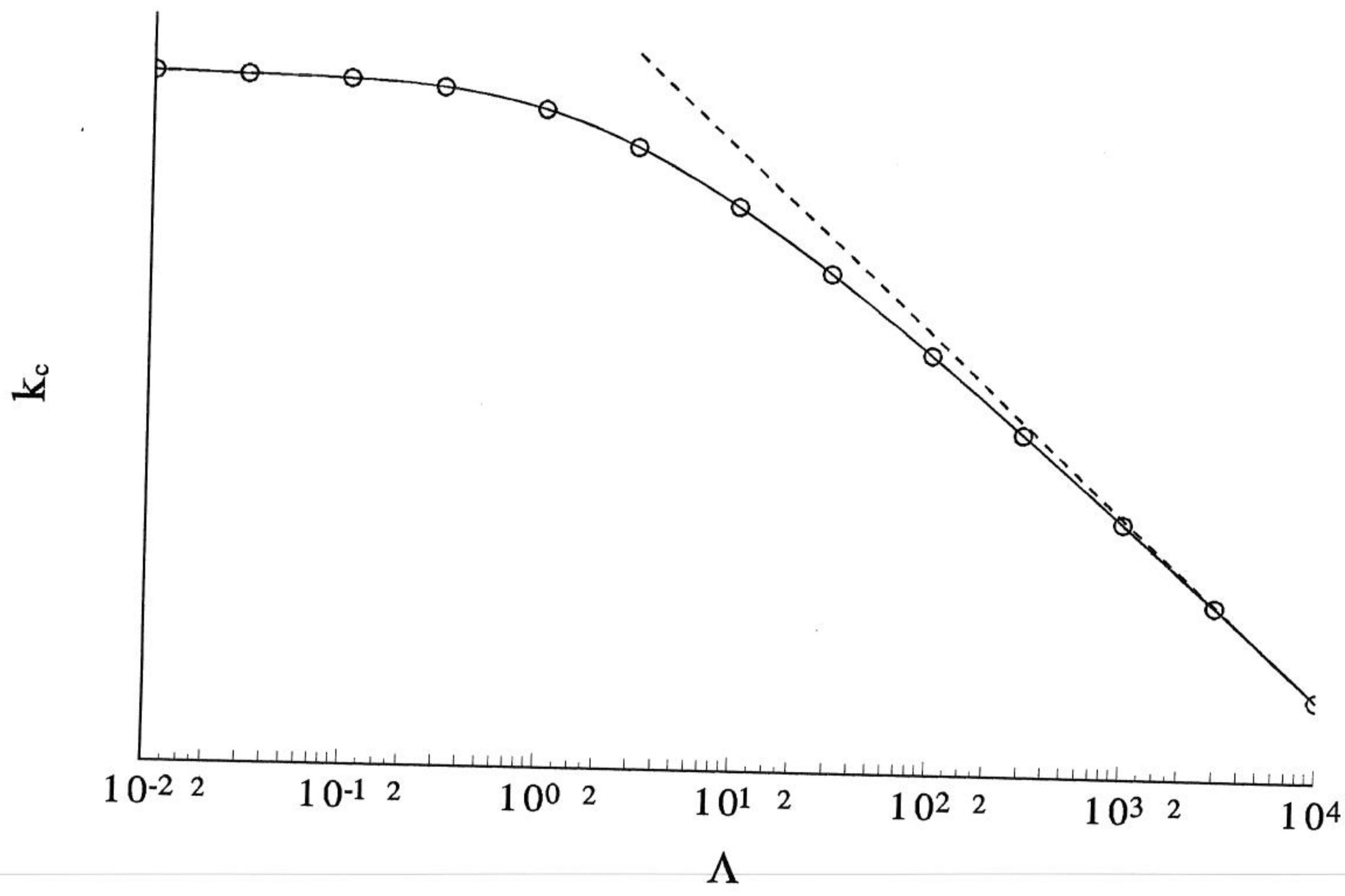

FIGURE 11(b)

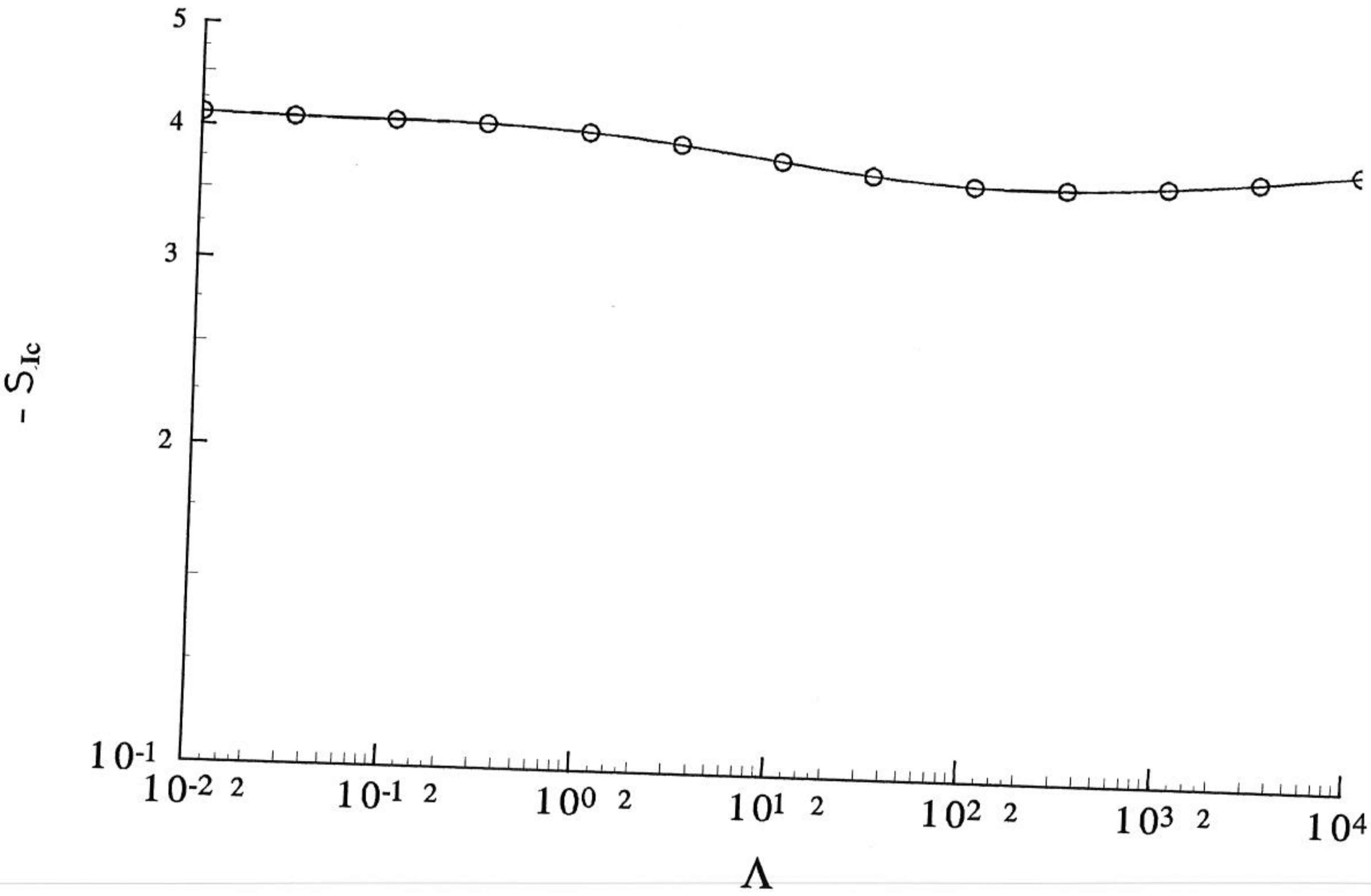

FIGURE 11(c)

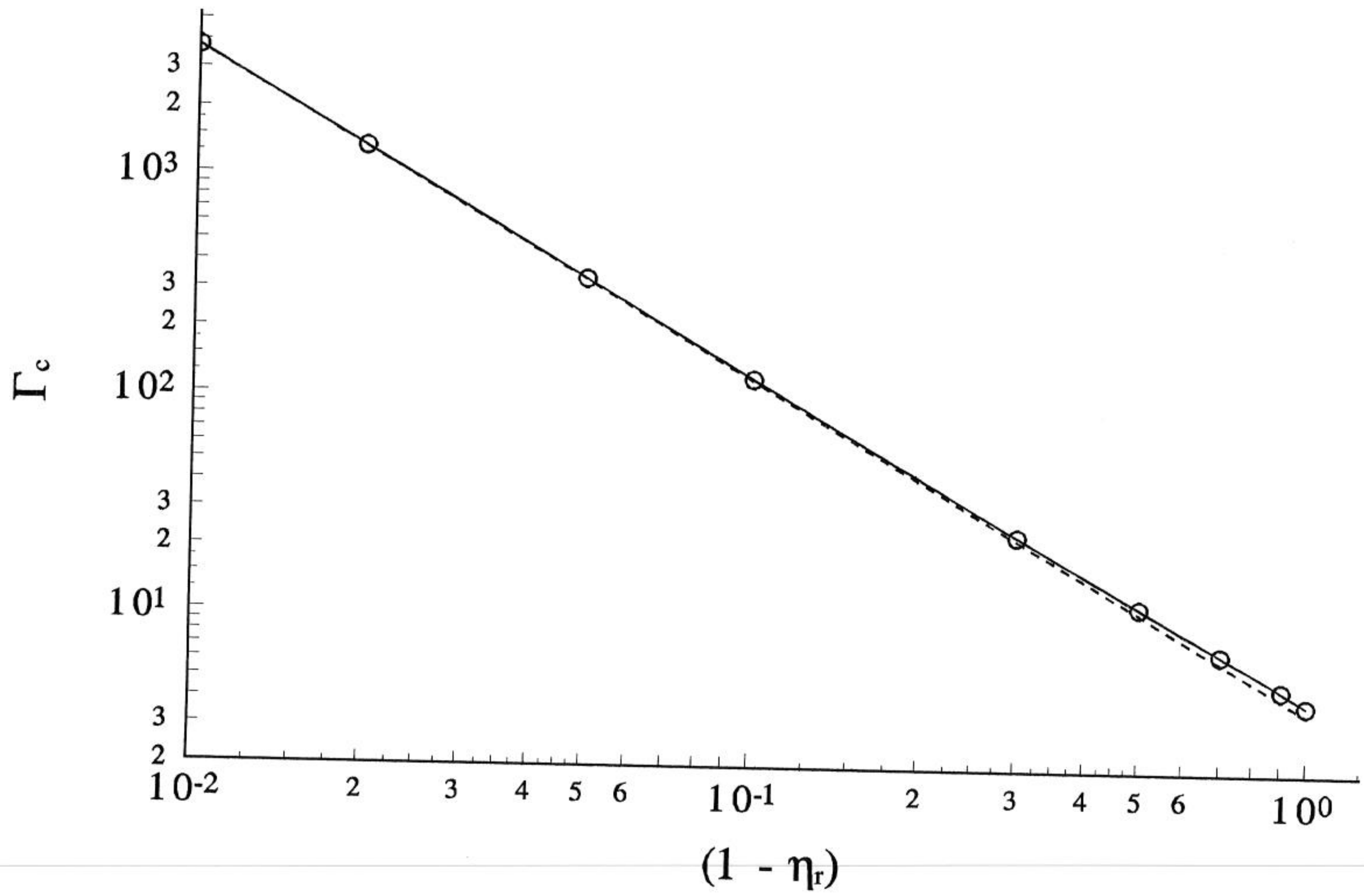

FIGURE 12(a)

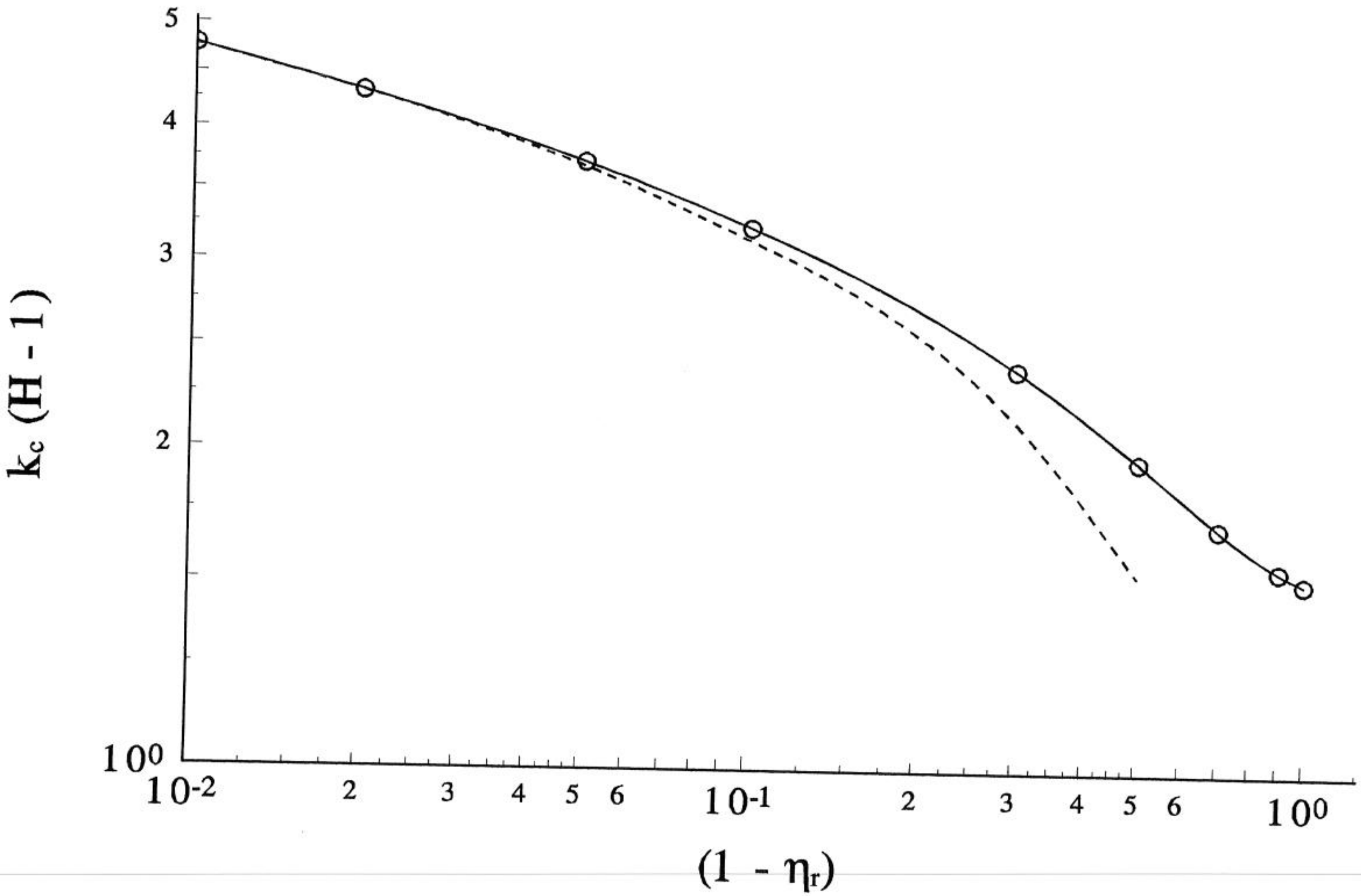

FIGURE 12(b)

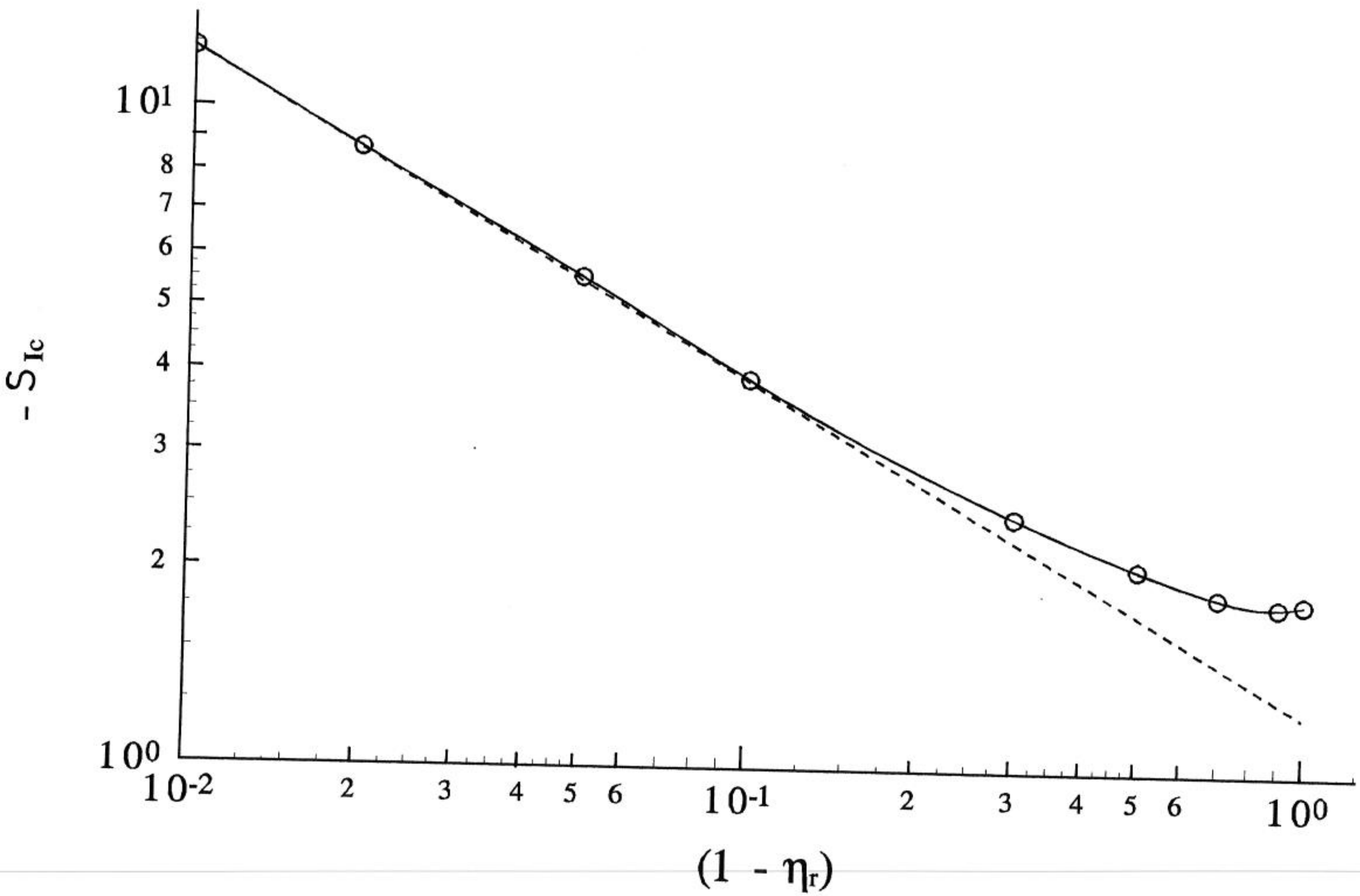

FIGURE 12(c)

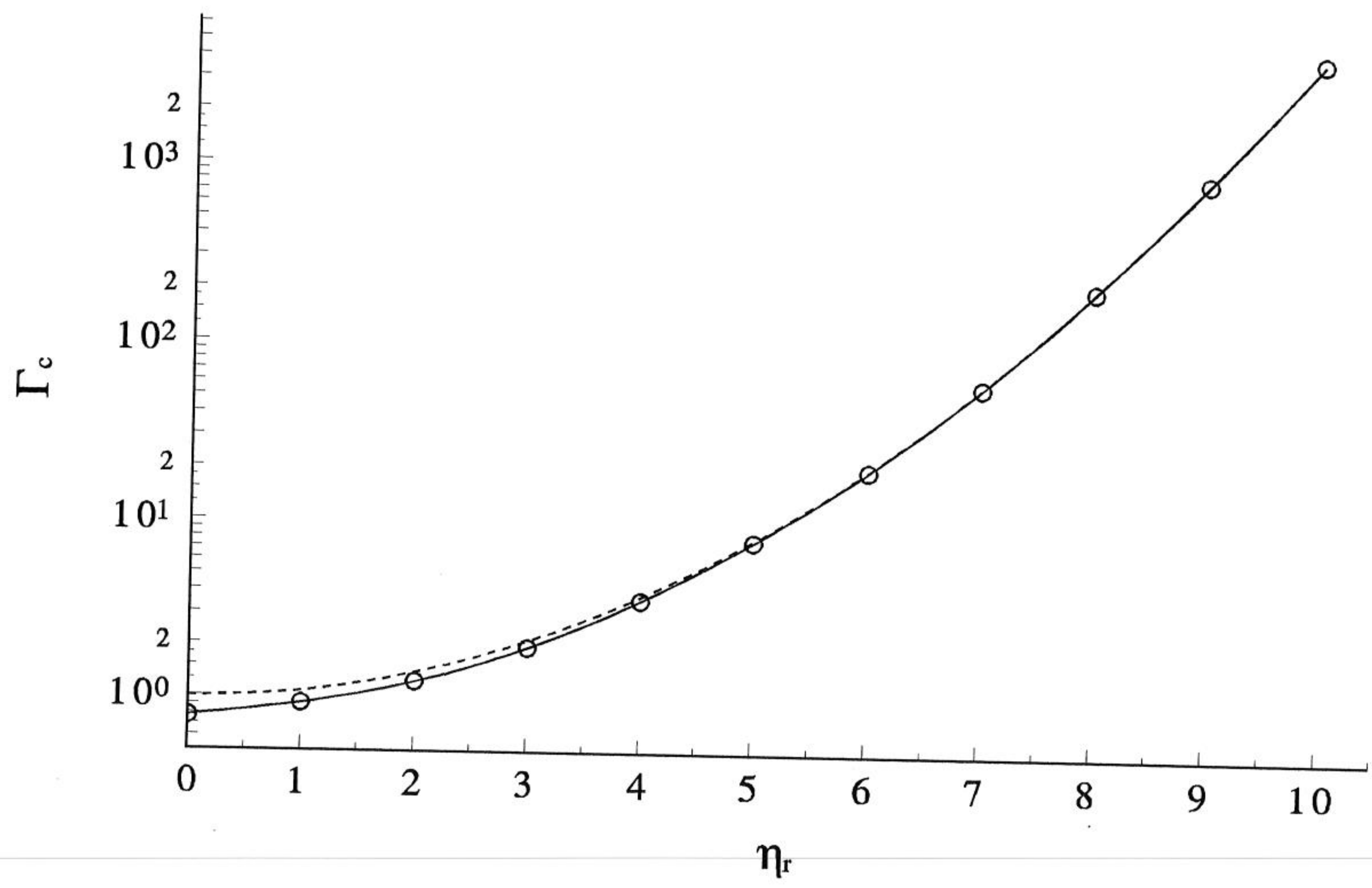

FIGURE 13(a)

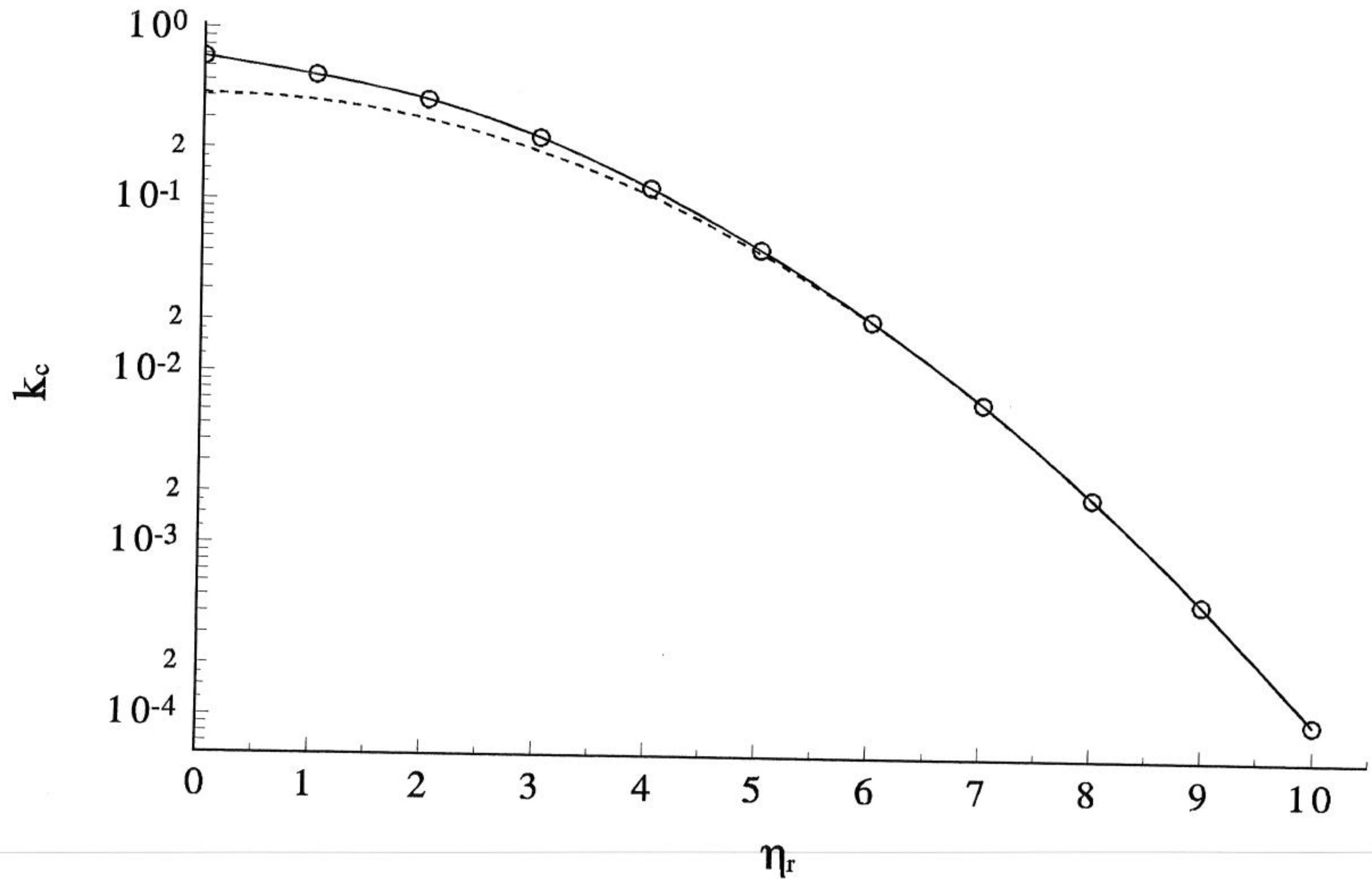

FIGURE 13(b)

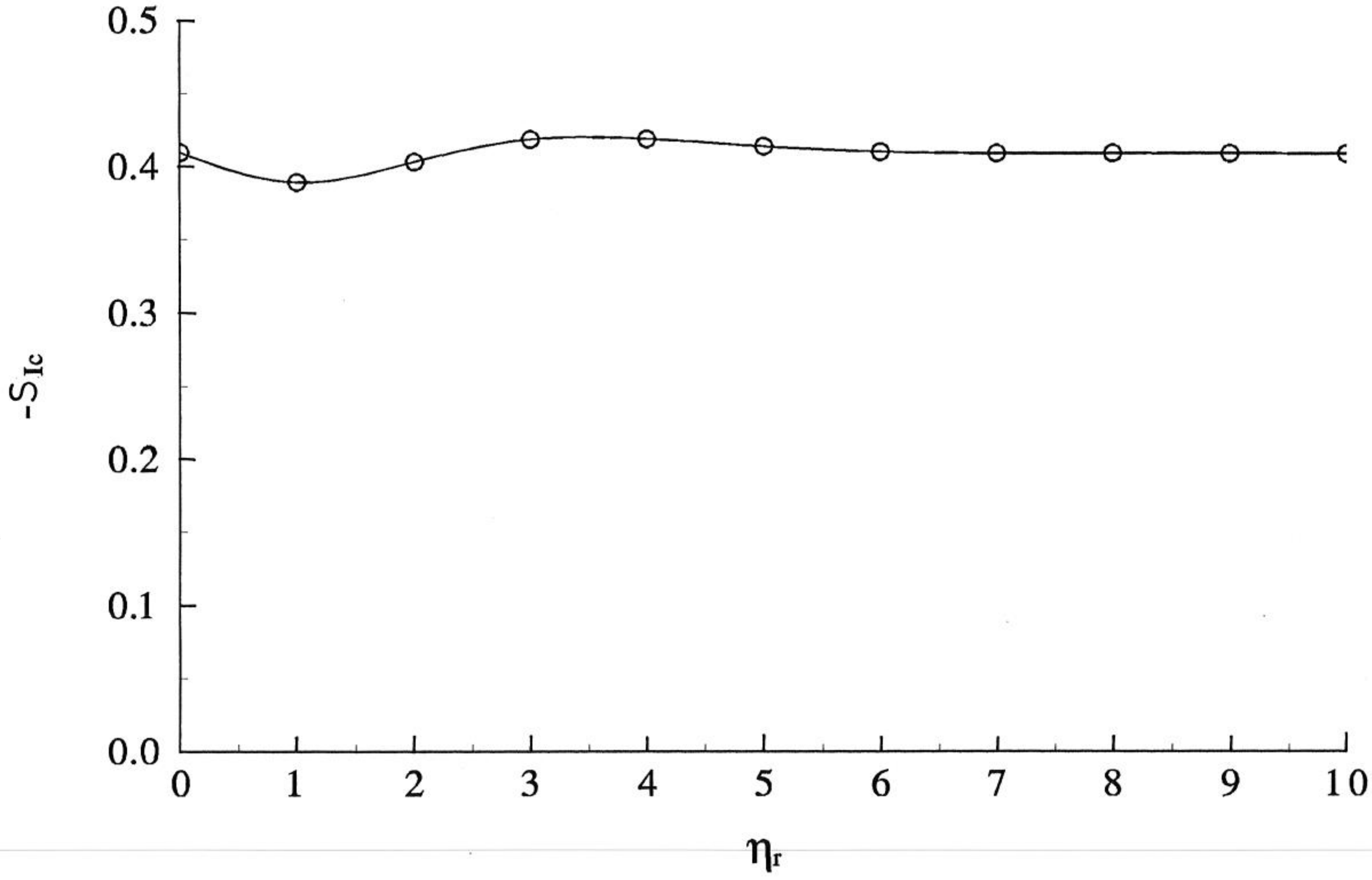

FIGURE 13(c)